Int. J. Heat Mass Transfer. Vol. 17, pp. 875–883. Pergamon Press 1974. Printed in Great Britain

TRANSIENT TEMPERATURE RESPONSE OF COMPOSITE SLABS

S. SUGIYAMA, M. NISHIMURA and H. WATANABE
Department of Chemical Engineering, University of Nagoya, Chikusa, Nagoya, Japan

(*Received* 14 *December* 1973)

Abstract—The general differential equations for unsteady uni-dimensional heat conduction in composite slabs were solved numerically by using the finite element method under the boundary conditions including the contact resistance between the layers.

The numerical results of transient temperature response agreed well with the analytical solution for the simple case and the experimental results for the various composite slabs. The effect of each factor on temperature response was clarified by examining the numerical and experimental results.

NOMENCLATURE

$B_{\mathrm{I}}, B_{\mathrm{II}}$,	Biot numbers, $B_{\mathrm{I}} = h_{\mathrm{I}} x_1/k_1$, $B_{\mathrm{II}} = h_{\mathrm{II}} x_1/k_1$;
c_p,	specific heat of material;
d,	thickness of material;
h_i,	heat-transfer coefficient due to contact resistance between ith layer and $(i+1)$th;
$h_{\mathrm{I}}, h_{\mathrm{II}}$,	heat-transfer coefficients between upper surface and surroundings, and lower surface and surroundings;
k,	thermal conductivity of material;
N,	number of subdivisions;
$q_{\mathrm{I}}, q_{\mathrm{II}}$,	heat fluxes at upper surface and lower;
T,	temperature;
T_{g1}, T_{g2},	ambient temperature;
t,	time;
x,	normal distance from upper surface to point.

Greek symbols

α,	thermal diffusivity of material;
β,	parameter for heating rate;
γ,	ratio of thermal conductivity, $= k_2/k_1$;
δ,	arbitrary constant;
ε,	emissivity of material;
ζ,	ratio of thickness, $= d_2/d_1 = (x_2 - x_1)/x_1$;
η,	ratio of thermal diffusivity, $= \alpha_2/\alpha_1$;
ξ,	dimensionless distance, $= x/x_1$;
ρ,	density of material;
σ,	Stefan–Boltzmann constant;
τ,	Fourier number, $= \alpha_1 t/x_1^2$;
ϕ,	dimensionless temperature.

Subscripts

i,	ith layer;
j,	jth subdivided point.

INTRODUCTION

IN THE design of the wall of industrial furnaces, chemical reactors and constructions, it is important to examine heat transfer through the composite wall as well as structural strength. Analytical results of heat transfer in steady state are often useful for many practical designs. The analysis of heat transfer in unsteady state, however, is necessary in considering the optimization of cyclic operations and starting up operations and similar problems.

The problem of heat transfer through the composite wall has been studied by Carslaw and Jaeger and many other investigators [1–7]. Few papers, however, have been published on heat transfer in unsteady state from the engineering viewpoint. Furthermore, the results in these papers may not be applied to practical engineering designs, because the theoretical analysis are restricted under the special conditions.

In this study, unsteady heat transfer through the composite slab of two or three layers was analysed under more general conditions. The basic differential equations for uni-dimensional heat conduction in the composite slab were derived in consideration of the temperature dependency of thermal properties of composing materials, and solved numerically by using a finite element method [8] under the boundary conditions including the contact resistance between layers. The variations with time of temperature distributions in the various composite slabs were measured under some boundary conditions, and the measurement results were compared with the calculated ones. In addition, the influence of each factor on temperature response and the availability of this analysis were discussed.

THEORETICAL ANALYSIS

As shown in Fig. 1, a composite slab is composed of n layers with different thermal properties. The differential equation for unsteady uni-dimensional heat

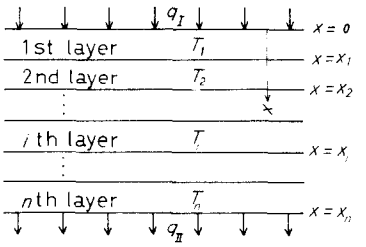

FIG. 1. Schematic diagram.

conduction in the ith layer may be expressed as

$$x_{i-1} \leqslant x \leqslant x_i;$$
$$c_{pi}\rho_i \frac{\partial T_i(x,t)}{\partial t} = \frac{\partial}{\partial x} k_i \frac{\partial T_i(x,t)}{\partial x} \quad i = 1, 2, \ldots, n. \quad (1)$$

The boundary conditions including the contact resistance between layers are given as follows

$$\left.\begin{aligned} &t > 0,\ x = x_0 = 0: \\ &\quad -k_1 \frac{\partial T_1(0,t)}{\partial x} = q_{\mathrm{I}} \\ &x = x_i: \\ &\quad -k_i \frac{\partial T_i(x_i,t)}{\partial x} = -k_{i+1} \frac{\partial T_{i+1}(x_i,t)}{\partial x} \\ &\qquad = h_i(T_i(x_i,t) - T_{i+1}(x_i,t)) \\ &\qquad\qquad (i = 1, 2, \ldots, n-1) \\ &x = x_n: \\ &\quad -k_n \frac{\partial T_n(x_n,t)}{\partial x} = q_{\mathrm{II}} \end{aligned}\right\} \quad (2)$$

where, q_{I} and q_{II} are heat fluxes due to convection and radiation at the surface $x = 0$, $x = x_n$, respectively, and h_i denotes the contact heat-transfer coefficient between the ith layer and the $(i+1)$th.

The initial conditions are

$$t = 0,\ 0 \leqslant x \leqslant x_n; \qquad T_i(x,0) = T_i(x). \quad (3)$$

It is impossible to solve equation (1) analytically under the conditions given by equations (2) and (3) in consideration of the temperature dependency of thermal properties. Therefore, equation (1) should be solved by a numerical method, and so the following finite element method was introduced in this study.

The Galerkin weighted residual process is used with equation (1) [8]. Multiplying both sides of equation (1) by an arbitrary continuous function $f_i(x)$ which is differentiable at least once, and integrating the resulting equation from x_{i-1} to x_i, we obtain

$$\int_{x_{i-1}}^{x_i} c_{pi}\rho_i \frac{\partial T_i(x,t)}{\partial t} f_i(x)\,\mathrm{d}x = \int_{x_{i-1}}^{x_i} \frac{\partial}{\partial x} k_i \frac{\partial T_i(x,t)}{\partial x} f_i(x)\,\mathrm{d}x$$
$$= \left[f_i(x) k_i \frac{\partial T_i(x,t)}{\partial x} \right]_{x_{i-1}}^{x_i} - \int_{x_{i-1}}^{x_i} k_i \frac{\partial T_i(x,t)}{\partial x} \frac{\partial f_i(x)}{\partial x}\,\mathrm{d}x. \quad (4)$$

The weighting function $f_i(x)$ shall be defined as follows:

$$x_{i-1} \leqslant x \leqslant x_i; \qquad f_i(x) \quad \sum_{j=0}^{N_i} \delta_{i,j} f_{i,j} \quad (5)$$

where

$$f_{i,0} = 1 - \frac{x - x_{i-1}}{s_i} \qquad (x_{i-1} \leqslant x \leqslant x_{i-1} + s_i)$$
$$= 0 \qquad (x < x_{i-1},\ x > x_{i-1} + s_i)$$
$$f_{i,j} = \frac{x - (j-1)s_i - x_{i-1}}{s_i}$$
$$(x_{i-1} + (j-1)s_i \leqslant x \leqslant x_{i-1} + js_i)$$
$$= \frac{(j+1)s_i + x_{i-1} - x}{s_i}$$
$$(x_{i-1} + js_i \leqslant x \leqslant x_{i-1} + (j+1)s_i)$$
$$= 0 \quad (x < x_{i-1} + (j-1)s_i,\ x > x_{i-1} + (j+1)s_i)$$
$$f_{i,N_i} = \frac{x - x_i + s_i}{s_i} \qquad (x_i - s_i \leqslant x \leqslant x_i)$$
$$s_i = \frac{x_i - x_{i-1}}{N_i}.$$

When T_i at the jth subdivided point is named $T_{i,j} (j = 0, 1, \ldots, N_i)$ and $T_i(x)$ is assumed to be linear with x in the interval $x_{i-1} + (j-1)s_i \leqslant x \leqslant x_{i-1} + js_i$, $T_i(x)$ is expressed as

$$x_{i-1} + (j-1)s_i \leqslant x \leqslant x_{i-1} + js_i;$$
$$T_i(x,t) = T_{i,j+1} \frac{x_{i-1} + js_i - x}{s_i} + T_{i,j} \frac{x - (j-1)s_i - x_{i-1}}{s_i}. \quad (6)$$

The values of c_{pi}, ρ_i and k_i in the temperature range $T_{i,j-1} \leqslant T_i(x) \leqslant T_{i,j}$ are approximated to those at the mean temperature $(T_{i,j-1} + T_{i,j})/2$, which are represented by $c_{pi,j}$, $\rho_{i,j}$ and $k_{i,j}$, respectively.

The rearrangement of equation (4) referred in Appendix gives the following ordinary differential equations.

$$\mathbf{C}\dot{\mathbf{T}} = \mathbf{A}\mathbf{T} + \mathbf{B} \quad (7)$$

where, $\mathbf{T}$, $\dot{\mathbf{T}}$ and $\mathbf{B}$ are column matrices, and $\mathbf{A}$ and $\mathbf{C}$ are tridiagonal matrices, all elements of which are shown in Appendix.

Now, $\mathbf{T}(t)$ and $\mathbf{T}(t+\Delta t)$ shall be denoted $\mathbf{T}$'s at time t and $t+\Delta t$, respectively. When $\mathbf{T}(t+\Delta t)$ is expanded

into a Taylor series about t and its terms higher than 3rd order are neglected, $\mathbf{T}(t+\Delta t)$ is expressed as

$$\mathbf{T}(t+\Delta t) = \mathbf{T}(t) + \Delta t\dot{\mathbf{T}}(t) + \frac{(\Delta t)^2}{2}\ddot{\mathbf{T}}(t). \quad (8)$$

The elimination of $\ddot{\mathbf{T}}(t)$ with both equation (8) and the equation obtained by differentiating equation (8) yields

$$\mathbf{T}(t+\Delta t) = \mathbf{T}(t) + \frac{\Delta t}{2}[\dot{\mathbf{T}}(t) + \dot{\mathbf{T}}(t+\Delta t)]. \quad (9)$$

In addition, equation (7) gives

$$\begin{aligned} \mathbf{C}^{(t)}\dot{\mathbf{T}}(t) &= \mathbf{A}^{(t)}\mathbf{T}(t) + \mathbf{B}^{(t)} \\ \mathbf{C}^{(t+\Delta t)}\dot{\mathbf{T}}(t+\Delta t) &= \mathbf{A}^{(t+\Delta t)}\mathbf{T}(t+\Delta t) + \mathbf{B}^{(t+\Delta t)}. \end{aligned} \quad (10)$$

With the assumption that $\mathbf{A}^{(t+\Delta t)} = \mathbf{A}^{(t)}$, $\mathbf{B}^{(t+\Delta t)} = \mathbf{B}^{(t)}$ and $\mathbf{C}^{(t+\Delta t)} = \mathbf{C}^{(t)}$ in equation (10), substitution of equation (10) into equation (9) yields

$$\mathbf{T}(t+\Delta t) = \mathbf{T}(t) + \frac{\Delta t}{2}\left[\{\mathbf{C}^{(t)}\}^{-1}\mathbf{X}(t) + \left\{\mathbf{C}^{(t)} - \frac{\Delta t}{2}\mathbf{A}^{(t)}\right\}^{-1} \times \left\{\mathbf{X}(t) + \frac{\Delta t}{2}\mathbf{A}^{(t)}\{\mathbf{C}^{(t)}\}^{-1}\mathbf{X}(t)\right\}\right] \quad (11)$$

where,

$$\mathbf{X}(t) = \mathbf{A}^{(t)}\mathbf{T}(t) + \mathbf{B}^{(t)}.$$

Equation (11) is the final form of the numerical solution of equation (1) obtained by using the finite element method. The procedure of the calculation of equation (11) is as follows: First, the column matrix $\mathbf{X}(0)$ is calculated by $\mathbf{T}(0)$, $\mathbf{A}^{(0)}$ and $\mathbf{B}^{(0)}$. Secondly, the temperature distribution at time Δt, $\mathbf{T}(\Delta t)$, is calculated from equation (11). Thirdly, $\mathbf{T}(2\Delta t)$ is calculated in the same manner. Thus, the variation with time of temperature distribution is obtained by repeating this procedure successively.

EXPERIMENTAL APPARATUS AND METHOD

The composite slab used for measurement was layers of flat discs of 300 mm in diameter. Each of the discs was different in thickness and thermal properties as tabulated in Table 1.

The outline of the experimental apparatus is shown in Fig. 2. The copper plate (500 mm square, 4 mm in thickness) was put on the upper surface of the composite slab, and the circinate nichrome wire heater of 2 kW in capacity was placed on the copper plate. The lower surface of the composite slab was exposed to air, and the side surface was insulated with insulation bricks and polystyrene foam. CA thermocouples of 0·1 mm in diameter and an automatic temperature recorder were used for temperature measurements. The temperature measurement points are shown in Fig. 2.

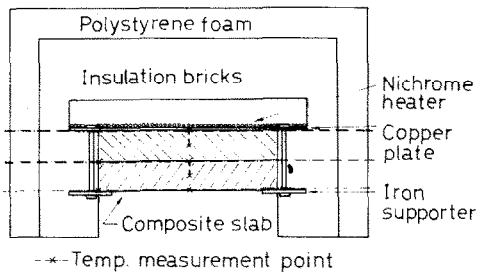

FIG. 2. Experimental apparatus.

The temperature in the slab was measured with the thermocouple which was placed in the hole of 1 mm in diameter drilled to the half of the thickness at the center. All the thermocouples were set in the cut of 1 × 1 mm made on the surface radially. In the heating experiment, heating rate was controlled manually with a slide-transformer, and the temperature rise of the lower surface of the copper plate was adjusted to the appointed heating curve:

$$T_H = T_{H\infty} - (T_{H\infty} - T_{H0})\exp(-\beta t)$$

where, $T_{H\infty} = 200°C$, $T_{H0} = 30°C$ and $\beta = 0{\cdot}9\,h^{-1}$. At the same time, the variations of temperature with time were measured at the above-mentioned points. In the cooling experiments, the composite slab was heated up to the steady state, and then cooled by sudden removal of the heater and the copper plate.

Table 1. Values of physical properties of composing materials

Material	Thickness $d(m)$	Density $\rho(kg/m^3)$	Specific heat $c_p(kcal/kg°C)$	Thermal conductivity $k(kcal/m\,h\,°C)$	Thermal diffusivity $\alpha(m^2/h)$	Emissivity ε
Gypsum board	0·019	870	0·26	0·1	$4{\cdot}4 \times 10^{-4}$	0·9
B1 insulation brick	0·03	660	0·20	0·17	$1{\cdot}3 \times 10^{-3}$	0·8
Low carbon steel	0·03	7800	0·11	40	$4{\cdot}7 \times 10^{-2}$	0·5

RESULTS

First, the accuracy of this numerical analysis was examined by comparing with the analytical solutions under the restricted conditions. Mayer [2] has solved analytically the problem of unsteady heat conduction in the composite slab of two layers under the following conditions: no flux across one surface and prescribed flux across the other surface, and neglect of contact resistance and the temperature dependency of thermal properties.

An example of comparison of this numerical solution with Mayer's solution is shown in Fig. 3 as for the composite slab of gypsum board and low carbon steel.

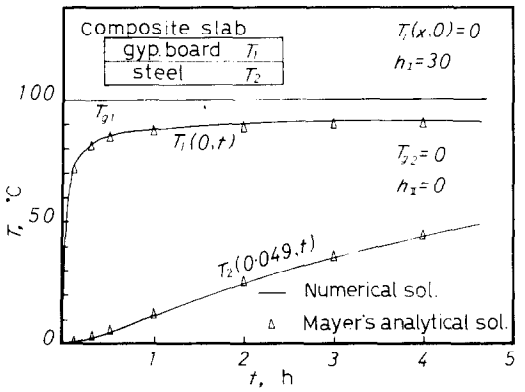

FIG. 3. Comparison of numerical solution with Mayer's solution.

In the numerical calculation, N_1 and N_2, the numbers of subdivisions, were 50 and 30, respectively, and Δt, the time interval, was $3{\cdot}0 \times 10^{-3}$ h.

As for the heating experiments, the comparisons of experimental results with numerical solutions are shown in Figs. 4–6. The composite slab of each figure was gypsum board–B1 insulation brick, gypsum board–low carbon steel and gypsum board–B1 insulation brick–low carbon steel. The other experimental conditions were $T_H = 200-170\exp(-0{\cdot}9t)$°C, $T_i(x,0) = 30$°C and $T_{g2} = 30$°C in every case. In addition, in these numerical calculations, the boundary conditions were given as follows:

$$\left.\begin{aligned} x = 0;\quad & q_{\mathrm{I}} = h_{\mathrm{I}}(T_H - T_1(0,t)) \\ x = x_n;\quad & q_{\mathrm{II}} = h_{\mathrm{II}}(T_n(x_h,t) - T_{g2}) \end{aligned}\right\}. \qquad (2')$$

In equation (2'), h_{I} can be considered to be the contact heat-transfer coefficient under this experimental condition. By using Weills and Ryder's correlation between the contact heat-transfer coefficient and the surface roughness [9], h_{I} in every case was assumed to be approximately 5000 kcal/m² h °C from the surface roughness of copper. For such a value, the difference between T_H and $T_1(0,t)$ was less than 0·2°C in Figs. 4–6. The heat-transfer coefficient h_{II} was given as follows:

$$h_{\mathrm{II}} = h_{\mathrm{II}c} + \varepsilon_{\mathrm{II}}\sigma\{T_n(x_n,t) + T_{g2} + 546{\cdot}0\} \times \{(T_n(x_n,t) + 273{\cdot}0)^2 + (T_{g2} + 273{\cdot}0)^2\}$$

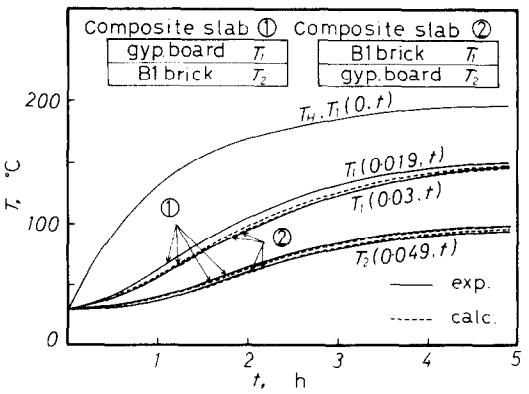

FIG. 4. Temperature response in heating of the composite slab (gypsum board–B1 insulation brick).

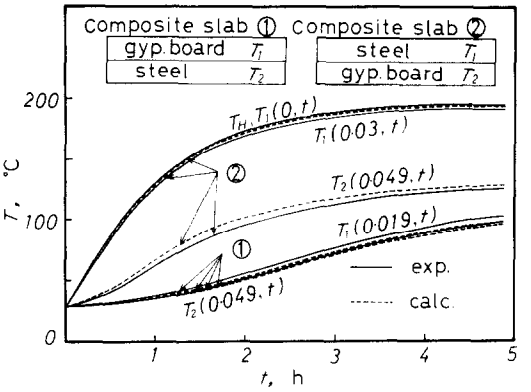

FIG. 5. Temperature response in heating of the composite slab (gypsum board–low carbon steel).

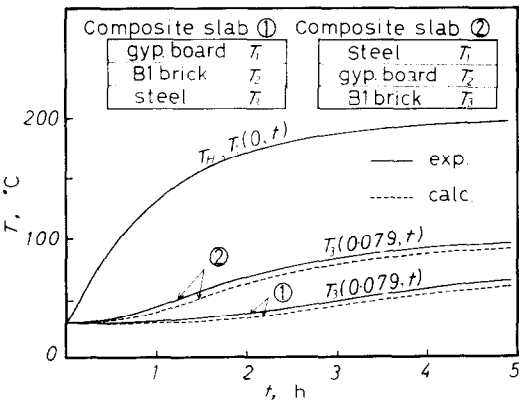

FIG. 6. Temperature response in heating of the composite slab (gypsum board–B1 insulation brick–low carbon steel).

where, $h_{\mathrm{II}c}$ is the heat-transfer coefficient due to natural convection, and its value was calculated from Fishenden and Saunder's correlation for a horizontal plate [10]. The contact heat-transfer coefficient h_i was assumed to be approximately 3000 kcal/m^2 h °C in every case. This is the value for steel obtained from the above-mentioned correlation. Furthermore, the temperature dependency of thermal properties was neglected, because the temperature variations were slight under this experimental condition.

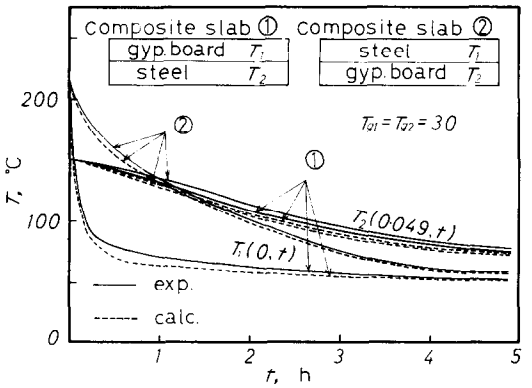

FIG. 7. Temperature response in cooling of the composite slab (gypsum board–low carbon steel).

As for the cooling experiments of the composite slab of gypsum board–low carbon steel, the comparison between both results is shown in Fig. 7. In this numerical calculation, both heat-transfer coefficients h_{I} and h_{II} were given in the same form as the above-mentioned h_{II}.

DISCUSSION

Accuracy of this numerical analysis

Figure 3 shows a good agreement between the numerical solution and the analytical one. The similar good agreements were also observed in the comparisons under other conditions. In addition, the moderate changes of the numbers N_1 and N_2 and the time interval Δt had little effect on the numerical solutions ($N_1 = 10$–60, $N_2 = 10$–40 for $\Delta t = 3{\cdot}0 \times 10^{-3}$ in Fig. 3).

From these facts, it is concluded that this numerical analysis using the finite element method has a good accuracy.

Furthermore, Figs. 4–7 show a fairly good agreement between the numerical solutions and the experimental results. It can be also concluded that this numerical analysis is useful for a problem of unsteady heat transfer through the composite slab under more general conditions.

Temperature response

In this section, temperature response is discussed in the relation of the location of the materials of which the composite slab is composed.

Figures 5 and 6 show a large difference in the manner of temperature response between the composite slab ① and ②. Namely, the unsteady temperature rises of the lower surface of ① in which the upper material has smaller thermal conductivity and thermal diffusivity are slower than that of ②, and there results a large difference of the rate of heat transfer between both the composite slabs. If the rate of radiant heat transfer at the lower surface is neglected, the steady temperature of the lower surface and the steady rate of heat transfer must be similar in both the composite slabs. In addition, the difference of the rate of radiant heat transfer between both the composite slabs has the reverse effect. Hence, such a difference can not be predicted from the steady temperature. As seen in Fig. 7, such a tendency is found similarly for the case of cooling experiments.

Figure 4, however, shows no remarkable difference between the composite slab ① and ②.

As predicted from the basic equations, such a difference in the manner of temperature response for the location may be dependent on the ratios of thickness, thermal conductivity and thermal diffusivity of the composing materials.

Now, we will further discuss the effects of non-dimensional parameters on temperature response on the basis of the results of the simplified numerical analysis.

With the assumptions of constant thermal properties and the neglection of contact resistance, the following dimensionless equations are obtained from equations (1), (2) and (3) for the composite slab of two layers.

$$\left.\begin{aligned} &0 \leqslant \xi \leqslant 1; \quad \frac{\partial \phi_1(\xi,\tau)}{\partial \tau} = \frac{\partial^2 \phi_1(\xi,\tau)}{\partial \xi^2} \\ &1 \leqslant \xi \leqslant 1+\zeta; \quad \frac{\partial \phi_2(\xi,\tau)}{\partial \tau} = \eta \frac{\partial^2 \phi_2(\xi,\tau)}{\partial \xi^2} \end{aligned}\right\} \quad (12)$$

$$\left.\begin{aligned} &\tau > 0,\ \xi = 0; \\ &\quad -\frac{\partial \phi_1(0,\tau)}{\partial \xi} = B_{\mathrm{I}}(\phi_{g1} - \phi_1(0,\tau)) \\ &\xi = 1; \\ &\quad -\frac{\partial \phi_1(1,\tau)}{\partial \xi} = -\gamma \frac{\partial \phi_2(1,\tau)}{\partial \xi}, \\ &\quad \phi_1(1,\tau) = \phi_2(1,\tau) \\ &\xi = 1+\zeta; \\ &\quad -\frac{\partial \phi_2(1+\zeta,\tau)}{\partial \xi} = \frac{B_{\mathrm{II}}}{\gamma}(\phi_2(1+\zeta,\tau) - \phi_{g2}) \end{aligned}\right\} \quad (13)$$

$$\tau = 0,\ \xi \geqslant 0; \quad \phi_1(\xi,0) = \phi_2(\xi,0) = \phi_i = 0 \quad (14)$$

where,

$$\phi_1 = (T_1(x,t) - T_1(x,0))/(T_{g1} - T_1(x,0)),$$
$$\phi_2 = (T_2(x,t) - T_1(x,0))/(T_{g1} - T_1(x,0)),$$
$$\tau = k_1 t/x_1^2 c_{p1}\rho_1 = \alpha_1 t/x_1^2, \quad \xi = x/x_1,$$
$$\zeta = (x_2 - x_1)/x_1, \quad \gamma = k_2/k_1,$$
$$\eta = c_{p1}\rho_1 k_2/c_{p2}\rho_2 k_1 = \alpha_2/\alpha_1,$$
$$B_{\mathrm{I}} = h_{\mathrm{I}} x_1/k_1, \quad B_{\mathrm{II}} = h_{\mathrm{II}} x_1/k_1.$$

In the meanwhile, the steady dimensionless temperature of the lower surface ($\xi = 1+\zeta$) is given as follows:

$$\phi_2(1+\zeta) = \phi_{g2} + \frac{1-\phi_{g2}}{B_{\mathrm{II}}\left(1+\frac{\zeta}{\gamma}+\frac{1}{B_{\mathrm{I}}}\right)+1}. \qquad (15)$$

Dimensionless temperature response was calculated for three combinations of parameters, η, ζ and γ, in the case $B_{\mathrm{I}} = 1000$, $B_{\mathrm{II}} = 0{\cdot}5$, $\zeta/\gamma = 1{\cdot}0$ and $\phi_2(1+\zeta) = 0{\cdot}5$. The results are shown in Figs. 8–10. It is found in three figures that the influence of η on dimensionless temperature response becomes remarkable at the larger values of ζ and γ. Also, from these figures, the effects of the location of materials on temperature response become more evident quantitatively. These results must be further discussed for the application to optimization of cyclic operation and starting up.

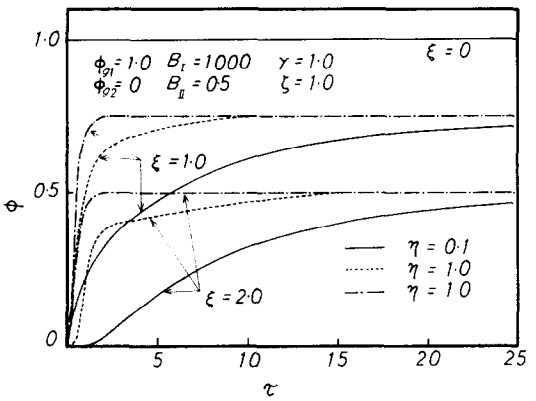

FIG. 8. Dimensionless temperature response for various thermal diffusivity ratios.

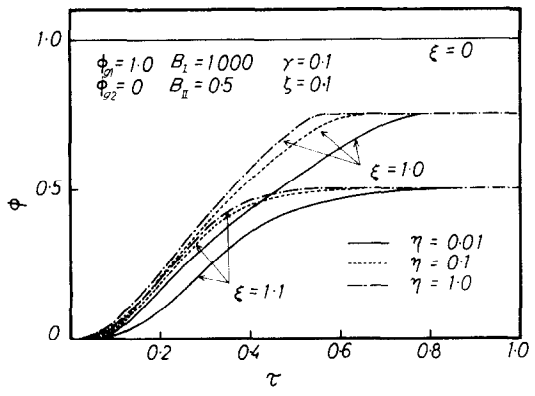

FIG. 9. Dimensionless temperature response for various thermal diffusivity ratios.

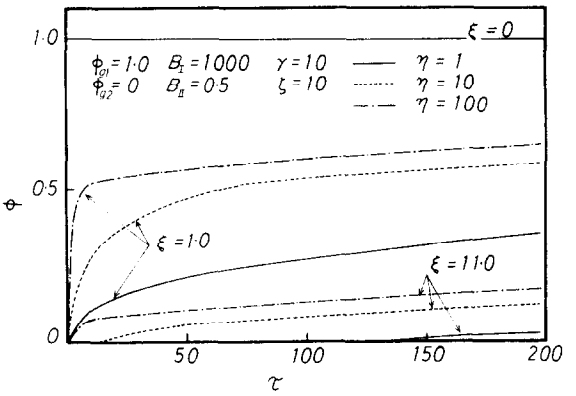

FIG. 10. Dimensionless temperature response for various thermal diffusivity ratios.

CONCLUSION

The basic differential equations for unsteady unidimensional heat conduction in the composite slab were derived in the general form, and solved numerically by the finite element method under the boundary conditions including the contact resistance between the layers.

The numerical results were observed to agree to both Mayer's analytical solution and the experimental results. It was concluded that this numerical analysis has a good accuracy and usefulness for such a problem. Also, the influence of each factor on temperature response became evident by examining the numerical and experimental results.

REFERENCES

1. H. S. Carslaw and J. C. Jaeger, *Conductance of Heat in Solid*, p. 319. Oxford University Press, New York (1947).
2. E. Mayer, Heat flow in composite slabs, *ARS Jl* **22**, 150–158 (1952).
3. W. P. Reid, Heat flow in composite slab, cylinder and sphere, *J. Franklin Inst.* **274**, 352–357 (1962).
4. W. P. Reid and E. Thomas, Calculation of temperature in a two-layer slab, *AIAA Jl* **1**, 2383–2384 (1963).
5. T. E. Stonecypher, Periodic temperature distribution in a two-layer composite slab, *J. Aero/Space Sci.* **27**, 152–153 (1960).
6. J. J. Brogan and P. J. Schneidar, Heat conduction in a series composite wall, *Trans. Am. Soc. Mech. Engrs* **83C**, 506–508 (1961).

7. Z. U. A. Warsi and N. K. Choudhury, Weighting function and transient thermal response of buildings—II. Composite structure, *Int. J. Heat Mass Transfer* **7**, 1323–1333 (1964).
8. O. C. Zienkiewicz, *The Finite Element Method in Engineering Science*, p. 38. McGraw-Hill, London (1971).
9. N. D. Weills and E. A. Ryder, Thermal resistance measurements of joints formed between stationary metal surfaces, *Trans. Am. Soc. Mech. Engrs* **71**, 259–267 (1949).
10. W. H. McAdams, *Heat Transmission*, 3rd Edn, p. 180. McGraw-Hill, New York (1954).

APPENDIX

The integrations of the term on the l.h.s. and the second term on the r.h.s. of equation (4) result in

$$\int_{x_{i-1}}^{x_i} c_{pi}\rho_i \frac{\partial T_i(x,t)}{\partial t} f_i(x)\,dx$$
$$= \delta_{i,0}\left\{\frac{c_{pi,1}\rho_{i,1}s_i}{3}\frac{\partial T_{i,0}}{\partial t} + \frac{c_{pi,1}\rho_{i,1}s_i}{6}\frac{\partial T_{i,1}}{\partial t}\right\} + \dots$$
$$+ \delta_{i,j}\left\{\frac{c_{pi,j}\rho_{i,j}s_i}{6}\frac{\partial T_{i,j-1}}{\partial t} + \frac{c_{pi,j}\rho_{i,j}s_i}{3}\frac{\partial T_{i,j}}{\partial t} + \frac{c_{pi,j+1}\rho_{i,j+1}s_i}{6}\frac{\partial T_{i,j+1}}{\partial t}\right\} + \dots$$
$$+ \delta_{i,N_i}\left\{\frac{c_{pi,N_i}\rho_{i,N_i}s_i}{6}\frac{\partial T_{i,N_i-1}}{\partial t} + \frac{c_{pi,N_i}\rho_{i,N_i}s_i}{3}\frac{\partial T_{i,N_i}}{\partial t}\right\} \quad \text{(A1)}$$

$$-\int_{x_{i-1}}^{x_i} k_i \frac{\partial T_i(x,t)}{\partial x}\frac{\partial f_i(x)}{\partial x}dx$$
$$= \delta_{i,0}k_{i,1}\frac{(-T_{i,0}+T_{i,1})}{s_i} + \dots$$
$$+ \delta_{i,j}\left\{\frac{k_{i,j}(T_{i,j-1}-T_{i,j})}{s_i} + \frac{k_{i,j+1}(-T_{i,j}+T_{i,j+1})}{s_i}\right\}$$
$$+ \dots + \delta_{i,N_i}k_{i,N_i}\frac{(T_{i,N_i-1}-T_{i,N_i})}{s_i}. \quad \text{(A2)}$$

The first term on the r.h.s. of equation (4) becomes

$$\left[f_1(x)k_1\frac{\partial T_1(x,t)}{\partial x}\right]_0^{x_1} = \delta_{1,N_1}k_{1,N_1}\frac{\partial T_{1,N_1}}{\partial x} - \delta_{1,0}k_{1,1}\frac{\partial T_{1,0}}{\partial x}$$
$$= \delta_{1,N_1}h_1(T_{1,N_1}-T_{2,0}) + \delta_{1,0}q_1$$

$$\left[f_i(x)k_i\frac{\partial T_i(x,t)}{\partial x}\right]_{x_{i-1}}^{x_i} = \delta_{i,N_i}k_{i,N_i}\frac{\partial T_{i,N_i}}{\partial x} - \delta_{i,0}k_{i,1}\frac{\partial T_{i,0}}{\partial x}$$
$$= \delta_{i,N_i}h_i(T_{i,N_i}-T_{i+1,0}) - \delta_{i,0}h_{i-1}(T_{i-1,N_i-1}-T_{i,0})$$

$$\left[f_n(x)k_n\frac{\partial T_n(x,t)}{\partial x}\right]_{x_{n-1}}^{x_n} = \delta_{n,N_n}k_{n,N_n}\frac{\partial T_{n,N_n}}{\partial x} - \delta_{n,0}k_{n,1}\frac{\partial T_{n,0}}{\partial x}$$
$$= -\delta_{n,N_n}q_{n+1} + h_{n-1}(T_{n-1,N_{n-1}}-T_{n,0}). \quad \text{(A3)}$$

After rearrangement of equation (4), use of the identity of $\delta_{i,j}$ gives

$$\mathbf{C}\dot{\mathbf{T}} = \mathbf{A}\mathbf{T} + \mathbf{B}$$

where,

$$\mathbf{A} = \begin{bmatrix}
-\frac{k_{1,1}}{s_1} & \frac{k_{1,1}}{s_1} & 0 & \cdots & 0 \\
\frac{k_{1,1}}{s_1} & -\frac{k_{1,1}+k_{1,2}}{s_1} & \frac{k_{1,2}}{s_1} & & \\
0 & & & & \\
 & & \frac{k_{i,N_i}}{s_i} & -\frac{k_{i,N_i}}{s_i}-h_i & h_i \\
 & & h_i & -\frac{k_{i+1,1}}{s_{i+1}}-h_i & \frac{k_{i+1,1}}{s_{i+1}} \\
 & & & & 0 \\
 & & & \frac{k_{n,N_n-1}}{s_n} & -\frac{k_{n,N_n-1}+k_{n,N_n}}{s_n} \quad \frac{k_{n,N_n}}{s_n} \\
0 & \cdots & 0 & & \frac{k_{n,N_n}}{s_n} \quad -\frac{k_{n,N_n}}{s_n}
\end{bmatrix}$$

$$\mathbf{C} = \begin{bmatrix} \frac{c_{p1,1}\rho_{1,1}s_1}{3} & \frac{c_{p1,1}\rho_{1,1}s_1}{6} & & & 0 & \cdots & 0 \\ \frac{c_{p1,1}\rho_{1,1}s_1}{6} & \frac{(c_{p1,1}\rho_{1,1}+c_{p1,2}\rho_{1,2})s_1}{3} & \frac{c_{p1,2}\rho_{1,2}s_1}{6} & & & & \\ 0 & \ddots & \ddots & \ddots & & & \\ & \frac{c_{pi,N_i}\rho_{i,N_i}s_i}{6} & \frac{c_{pi,N_i}\rho_{i,N_i}s_i}{3} & 0 & & & \\ & 0 & \frac{c_{pi+1,1}\rho_{i+1,1}s_{i+1}}{3} & \frac{c_{pi+1,1}\rho_{i+1,1}s_{i+1}}{6} & & & \\ & & \ddots & \ddots & \ddots & & 0 \\ & & & \frac{c_{pn,N_n-1}\rho_{n,N_n-1}s_n}{6} & \frac{(c_{pn,N_n-1}\rho_{n,N_n-1}+c_{pn,N_n}\rho_{n,N_n})s_n}{3} & \frac{c_{pn,N_n}\rho_{n,N_n}s_n}{6} & \\ 0 & \cdots & 0 & & \frac{c_{pn,N_n}\rho_{n,N_n}s_n}{6} & \frac{c_{pn,N_n}\rho_{n,N_n}s_n}{3} & \end{bmatrix}$$

$$\mathbf{B} = \begin{bmatrix} q_{\mathrm{I}} \\ 0 \\ \vdots \\ 0 \\ q_{\mathrm{II}} \end{bmatrix}, \quad \mathbf{T} = \begin{bmatrix} T_{1,0} \\ T_{1,1} \\ \vdots \\ T_{i,j} \\ \vdots \\ T_{n,N_n-1} \\ T_{n,N_n} \end{bmatrix}, \quad \dot{\mathbf{T}} = \begin{bmatrix} \dot{T}_{1,0} \\ \dot{T}_{1,1} \\ \vdots \\ \dot{T}_{i,j} \\ \vdots \\ \dot{T}_{n,N_n-1} \\ \dot{T}_{n,N_n} \end{bmatrix}.$$

REPONSE TRANSITOIRE EN TEMPERATURE DES PLAQUES COMPOSITES

Résumé—On résout numériquement les équations aux dérivés partielles générales de la conduction thermique unidirectionnelle dans des plaques composites, en utilisant la méthode des éléments finis avec des conditions aux limites incluant la résistance de contact entre les couches.

Les résultats numériques concernant la température transitoire s'accordent bien avec la solution analytique du cas simple et avec les résultats expérimentaux obtenus pour différentes plaques composites. L'effet de chaque facteur sur la réponse en température est dégagé en examinant les résultats numériques et expérimentaux.

TEMPERATURAUSGLEICH IN GESCHICHTETEN PLATTEN

Zusammenfassung—Die Differentialgleichungen für instationäre eindimensionale Wärmeleitung in geschichteten Platten wurden in allgemeiner Form mit Hilfe der Methode finiter Elemente unter Randbedingungen gelöst, die den Kontaktwiderstand zwischen den Schichten einschließen.

Die Ergebnisse der numerischen Lösung stimmten gut mit der analytischen Lösung für den einfachen Fall und mit experimentellen Ergebnissen für verschiedene, geschichtete Platten überein. Die Auswirkung jeder Einflußgröße auf den Temperaturverlauf wurde durch Analysieren der rechnerischen und experimentellen Ergebnisse geklärt.

НЕСТАЦИОНАРНАЯ ТЕМПЕРАТУРНАЯ ХАРАКТЕРИСТИКА СОСТАВНЫХ ПЛИТ

Аннотация — С помощью метода конечных элементов получено численное решение общих дифференциальных уравнений нестационарной одномерной теплопроводности в составных плитах при граничных условиях, учитывающих контактное сопротивление между слоями.

Найдено, что численные результаты по нестационарной температурной характеристике хорошо согласуются с аналитическим решением для простого случая и с экспериментальными результатами для различных составных плит. На основе анализа численных и экспериментальныхрезультатов уточнено влияние каждого фактора на температурную характеристику.